

## Research Article

# Effect of Structural Transformations on Precipitability and Polarity of Red Wine Phenolic Polymers

Ingrid Weilack,<sup>1</sup> Christina Schmitz,<sup>1</sup> James F. Harbertson,<sup>2,3</sup> Fabian Weber<sup>1\*</sup>

<sup>1</sup>Institute of Nutritional and Food Sciences, Molecular Food Technology, University of Bonn, Endenicher Allee 19b, D 53115 Bonn, Germany; <sup>2</sup>Washington State University, 2710 University Drive, Richland, WA 99354-7224; and <sup>3</sup>Associate Professor of Enology, Washington State University, Viticulture and Enology Program, School of Food Science.

\*Corresponding author (fabian.weber@uni-bonn.de; tel: +49-228-734462; fax: +49-228-734429)

This research project was financially supported by the German Ministry of Economics and Technology (via AiF) and the FEI (Forschungskreis der Ernährungsindustrie e.V., Bonn). Project AiF 20024 N.

Manuscript submitted Oct 20, 2020, revised Jan 19, 2021, accepted Feb 5, 2021

Copyright © 2021 by the American Society for Enology and Viticulture. All rights reserved.

By downloading and/or receiving this article, you agree to the Disclaimer of Warranties and Liability. The full statement of the Disclaimers is available at <http://www.ajevonline.org/content/proprietary-rights-notice-ajev-online>. If you do not agree to the Disclaimers, do not download and/or accept this article.

**Abstract:** Condensed tannins and polymeric pigments are essential red wine components since they contribute to color stability, taste, and mouthfeel. Phenolic polymers in red wine consist of flavan-3-ol monomers as well as anthocyanins and cause the perception of astringency. Due to the chemical heterogeneity of proanthocyanidin polymers, analytical tools for the determination of the polymers' structural features are limited. The incorporation of anthocyanins increases the structural complexity even more and leaves it almost impossible to assess the influence of structure on the evoked astringency. To obtain a better understanding of the structural diversity of red wine polymers, this study combines forced aging and the FLASH-fractionation of polyphenolic wine extracts to reveal the relationship between phenolic polymers and two physicochemical properties, polarity, and hydrophilicity. Red wine fractions were characterized regarding their polarity,

octanol-water partitioning coefficient, protein precipitation assay, UHPLC-MS, and color. Tannin concentrations in wine decreased during forced aging while the concentrations were constant in the corresponding extracts, suggesting an alteration of the precipitation behavior. A simultaneous increase of precipitable polymeric pigments gives rise to the assumption that the incorporation of anthocyanins into tannin molecules alters the interactions with red wine polysaccharides and proteins, which results in lower tannin readings. Finding tannins and polymeric pigments in different FLASH-fractions indicates that precipitability of polymers is affected by the physicochemical properties, which in turn depend on the degree of polymerization as well as degree of pigmentation. The results of this study show that red wine astringency and its sub-qualities may be related to the increase in precipitable polymeric pigments during forced red wine aging and their putative enhanced interaction with wine polysaccharides and can help to better understand astringency mechanisms.

**Key words:** interactions, physicochemical, pigmentation, polymers, red wine, tannins

## Introduction

Phenolic compounds are essential components of wine and anthocyanins and flavan-3-ols are arguably of utmost importance for red wine quality since they contribute to color and its stability as well as taste and mouth-feel properties (Cheynier et al. 2006). While monomeric flavan-3-ols contribute to bitterness, tannins and oligomeric proanthocyanidins are largely responsible for the perception of astringency (Gawel 1998, Noble 1998). The composition of the tannins, expressed by the degree of polymerization and galloylation as well as the number of trihydroxylated monomers, are the driving forces for the intensity and quality of astringency

perception, which is explained by a loss of lubrication as a result of polyphenols precipitating saliva proteins (Noble 1998, de Freitas and Mateus 2001, Vidal et al. 2003, Harbertson et al. 2014). Anthocyanins determine the color of young red wines and are extracted during wine making. They have a key role in the modulation of color and mouthfeel properties during red wine aging.

Anthocyanins are transformed to more stable pigments which is accompanied by a loss in wine color density (Bindon et al. 2014). Together with some low molecular wine constituents and yeast metabolites, anthocyanins can form pyranoanthocyanins (Fulcrand et al. 2006) or can be incorporated into tannin-like structures. Tannins that incorporate anthocyanins during red wine aging are designated polymeric pigments (Remy et al. 2000).

Chira et al. (2012) reported an age-related decrease of tannin concentrations and mean degree of polymerization (mDP) accompanied with a decline in perceived astringency. In contrast, McRae et al. (2012) showed that tannin concentrations were not directly related to wine age and that tannin size increased during aging indicating that lower astringency ratings of aged wines do not result solely from lower tannin concentrations and mDPs. Earlier studies (Vidal et al. 2004a, Weber et al. 2013) suggested that the formation of polymeric pigments found in aged red wine attenuates astringency. Hence, the incorporation of anthocyanins may affect astringency perception even more than the concomitant increasing polymer length.

Due to similar chemical structures and the chemical heterogeneity of proanthocyanidin polymer length, sub-unit composition, and constitution, analysis of these phenolics has proved difficult. Reversed-phase HPLC-DAD-MS is commonly used to identify and quantify low molecular polyphenols, but this approach is limited regarding tannin analysis since they elute as a polydisperse hump (Ma et al. 2018). Methods that are utilized to partly characterize red wine

polymers include tannin precipitation either by proteins in combination with bisulfite bleaching (Harbertson et al. 2002, 2003) or polysaccharides (Sarneckis et al. 2006). Acid-catalyzed cleavage of proanthocyanidins in the presence of nucleophilic agents like phloroglucinol (Kennedy and Jones 2001) is another approach to assess polymer composition. However, this method showed its limits when applied to analyze pigmented tannins (Vidal et al. 2004a) and therefore, the manifold structures of polymeric pigments have not yet been identified. Consequently, the complex composition and alteration of red wine polymers as well as their impact on astringency perception remain important issues to be studied.

To address this lack of knowledge, this study utilizes normal-phase FLASH-chromatography to fractionate red wine polyphenols according to their size and polarity. The fractions were chemically characterized including the determination of their octanol-water partitioning coefficients ( $K_{OW}$ ) to measure hydrophilicity. A previous study (Merrell et al. 2018) showed that the  $K_{OW}$  is influenced by tannin composition and red wine maturity. Combining forced aging and fractionation of polyphenolic wine extracts aims at revealing the relationship between polymeric pigments as well as tannins and two physicochemical properties. Polarity and hydrophilicity were investigated to gain a better understanding of the structural diversity of red wine polymers.

## Materials and Methods

### *Materials*

Acetic acid, hexane, hydrochloric acid (HCl), potassium bisulfite, and acetonitrile were purchased from VWR International GmbH (Darmstadt, Germany). Ethanol, bovine serum albumin

fraction V, and (+)-Catechin were purchased from Carl Roth (Karlsruhe, Germany). Silica gel 60 Å (particle size 0.063-0.2 mm, 70-230 mesh) and sodium hydroxide were purchased from Honeywell Fluka (Offenbach, Germany). Urea, maleic acid, ferric chloride, triethanolamine (TEA), and octanol were purchased from Alfa Aesar (Kandel, Germany). Sodium chloride and Amberlite XAD7 were purchased from Labochem int. (Heidelberg, Germany) and Sigma-Aldrich (Darmstadt, Germany), respectively.

#### *Wine samples*

Two different commercially available wines were chosen in this study. Six bottles each of the 2018 Cabernet Sauvignon from the Trapiche winery (Maipú, Mendoza, Argentina) and the 2016 Cabernet Sauvignon from the Salentein winery (Tunuyán, Mendoza, Argentina) were used. The wines were assessed in advance by FT-IR and in a bench tasting, which verified that both wines had no considerable differences in their general composition and sensory properties. Two different wines from two vintages were selected to investigate whether wine phenolic composition and tannin structures change differently in an older wine compared to a younger wine during forced aging. The 2018 wine was composed as follows: 13% ethanol by volume, 9 g/L glycerol, pH 3.7, titratable acidity as 5.9 g/L tartaric acid equivalents, 5 g/L residual sugars, 1935 mg/L catechin equivalents total phenolic content. The 2016 wine was composed as follows: 13.5% ethanol by volume, 10 g/L glycerol, pH 3.8, titratable acidity as 5.4 g tartaric acid equivalents/L, 5 g/L residual sugars, 2117 mg/L catechin equivalents total phenolic content. Apart from the phenolic content, that was determined according to chapter 2.5, these parameters were obtained using Fourier-transform mid-infrared spectroscopy, including the appropriate calibration method (WineScan FT120 Basic, Foss, Hilleroed, Denmark). The total phenolic contents of the wines were not

significantly different at  $p \leq 0.05$ . Free and total  $\text{SO}_2$  values were 6 mg/L and 70 mg/L for the 2016 wine and 10 mg/L and 100 mg/L for the 2018 wine determined by titration. The samples were split into three pairs. Two were kept at 35 °C for three or six weeks and were compared to the non-aged wines. All bottles were closed with screw caps and the two bottles of each sample were pooled for all experiments.

#### *Solid phase extraction and fractionation of phenolic compounds*

To obtain a polyphenol rich extract from the wines, each wine sample was diluted with water (1:2) and was loaded onto an Amberlite XAD7 column (65 mm x 450 mm; 1.5 L bed volume), which was previously washed with 250 mL of a 0.1% (w/v) sodium hydroxide solution and preconditioned with 2 L of water. After elution of the wine, the column was washed with 2 L of water (1.3 fold of the bed volume) in order to remove sugars and organic acids. The polyphenols were eluted with approximately 3 L of ethanol acidified with acetic acid (29:1 v/v) at a gravity flow rate of approximately 10 mL/min. The collected extracts were concentrated using a rotary evaporator and consecutively lyophilized. The fractionation was conducted on a self-packed silica gel 60 Å column (36 mm x 460 mm; 0.5 L bed volume) using a low-pressure chromatography pump (C-605 pump with C-615 pump manager, Büchi Labortechnik GmbH, Essen, Germany). Isocratic elution involved three solvents: 60% hexane, 40% ethanol (solvent A), ethanol with 1% formic acid (solvent B), and 50% ethanol (v/v) with 1% formic acid (solvent C). At a flow rate of 90 mL/min the column was first rinsed with solvent C for 10 minutes and then preconditioned with solvent A for another 10 minutes. Subsequently, 5 mL of extract dissolved in solvent B were loaded onto the column with a concentration of 75 g/L. Solvent A, B and C were successively applied to the column for 10 minutes each and changed manually. Elution was monitored at 280 nm and 520

nm with a Knauer BlueShadow 50D detector and the ClarityChrom Software (Knauer, Berlin, Germany). According to the chromatogram obtained at 280 nm, the fractions were manually combined. After complete elution, solvents were evaporated, and the fractions were lyophilized. The column was washed with solvent C for 10 minutes. Prior to further analyses, the lyophilized fractions and extracts were dissolved at concentrations of 2 g/L in a wine-like solution (12% ethanol by volume, 5 g/L tartaric acid, pH 3.3 adjusted with NaOH).

#### *Spectrophotometric analysis*

Absorbance spectra were recorded in undiluted wines and sample solutions between 300 and 800 nm by a Jasco V-730 double-beam spectrophotometer (JASCO Deutschland GmbH, Pfungstadt, Germany), using a 1 mm path-length glass cuvette (Hellma GmbH & Co. KG, Müllheim, Germany). After values were corrected to a 10 mm path length cylindrical coordinates chroma C\* and hue h\* were calculated with the Spectra Manager Ver.2.14G (JASCO Deutschland GmbH, Pfungstadt, Germany) according to OIV recommendations (OIV 2006).

#### *Chemical characterization*

Anthocyanins were analyzed following the protocol reported by Harbertson et al. (2009). Protein precipitation was combined with bisulfite bleaching to determine tannins and polymeric pigments (Harbertson et al. 2002, 2003) using a reformulated resuspension buffer (urea 8.3 M, 5% TEA, pH 7 adjusted with HCl) as published by Harbertson et al. (2015). To quantify total iron reactive phenolics, an aliquot of the sample is diluted with the previously mentioned resuspension buffer to a total volume of 875 µL and incubated for 10 minutes. Absorbance at 510 nm is measured before and after addition of 125 µL of ferric chloride solution. Tannins and total iron

reactive phenolics were expressed as catechin equivalents (CE) according to an external calibration curve.

#### *Octanol-Water partition coefficient*

A volume of 1 mL of the sample solution was thoroughly mixed with 1 mL of octanol and vortexed for 10 seconds. For faster separation of the phases, the samples were centrifuged at 9,600g for 10 minutes. Subsequently, an aliquot of both phases was injected into the Shimadzu Nexera X2 UHPLC-DAD system (two Nexera X2 LC-30AD high-pressure gradient pumps, a Prominence DGU-20A5R degasser, a Nexera SIL-30AC autosampler (15 °C, injection volume 2 µL), a CTO-20AC Prominence column oven (40 °C), and a SPD-M20A Prominence diode array detector; Shimadzu, Kyoto, Japan) using an ACQUITY HSS T3 column (50 mm × 2.1 mm, 1.8 µm; Waters, Milford, USA). At a flow rate of 0.5 mL/min samples were eluted using the following gradient: 0 min, 50% B; 2 min, 100% B; 3.3 min, 100% B; 4 min, 50% B; 7 min, 50% B, with A being water/formic acid (97/3; v/v) and B being acetonitrile/formic acid (97/3; v/v). The partitioning coefficient was formed by the ratio of the samples' total peak area in the octanol phase and the water phase, respectively, according to the chromatogram at 280 nm.

#### *UHPLC-ESI-MS/MS*

UHPLC-MS analysis of the fractions was performed on an Acquity UPLC I-Class system (Waters, Milford, MA) consisting of a binary pump, an autosampler cooled at 10 °C, a column oven set at 40 °C, and a diode array detector scanning from 190 to 800 nm. An Acquity HSS-T3 RP18 column (150 × 2.1 mm; 1.8 µm particle size) combined with a precolumn (Acquity UPLC HSS T3 VanGuard, 100 Å, 2.1 × 5 mm, 1.8 µm), both from Waters (Milford, MA) was used for



separation. At a flow rate of 0.5 mL/min analytes were eluted using the following gradient: 0 min, 5% B; 8 min, 10% B; 25 min, 25% B; 26 min, 100% B; 28 min, 100% B; 29 min, 5% B; 31 min, 5% B, with A being water/formic acid (97/3; v/v) and B being acetonitrile/formic acid (97/3; v/v). The injection volume was 5  $\mu$ L. The UPLC was coupled to a LTQ-XL ion trap mass spectrometer (Thermo Scientific, Inc., Waltham, MA) equipped with an electrospray interface operating in positive ion mode for analysis of anthocyanins and anthocyanin derivatives and in negative ion mode for other polyphenols. For identification, mass spectra were recorded in the range of  $m/z$  120–1500 with three consecutive mass scans ( $MS^2$ , 35% normalized collision energy;  $MS^3$ , 45% normalized collision energy). The capillary was set at 325 °C with a voltage of 40 V for  $ESI^+$ , and at 350 °C and a voltage of –44 V for  $ESI^-$ . The source voltage was maintained at 5 and 4 kV, respectively, at a current of 100  $\mu$ A. The tube lens was adjusted to 70 V for  $ESI^+$  and –105 V for  $ESI^-$ . For quantification, specific  $m/z$  values of 63 polyphenolic compounds were recorded in single ion monitoring (SIM) measurements using one scan event.

### *Sensory analysis*

To determine the effects of alterations of tannin structures on astringency during forced aging, overall astringency of the wines was evaluated by a panel tasting. The sensory panel was composed of 14 volunteer judges that participated in three training sessions prior to the final tasting. The first session was dedicated to the differentiation between astringency, sourness and bitterness by the panelists who were familiarized with these tastes and sensations. Solutions of aluminum sulfate (2 g/L), caffeine (1.5 g/L) and tartaric acid (2 g/L) in a Pinot noir wine from 2018 used as basic wine were presented to train astringency, bitterness, and sourness perception.

The second session was dedicated to the recognition of various aluminum sulfate concentrations (0, 0.5, 1 and 2 g/L). Panelists were advised to rank the standard solutions by ascending intensity. During the third session the panelists were introduced to the intensity scale of the final tasting which was a structured scale from 1 to 10 for “very low intensity” and “very high intensity”, respectively. Two astringency standard solutions (0.5 g/L and 3 g/L) were presented and set as points 3 and 8 of the scale after panel discussion. The final tasting was held in four individual sessions and three samples were evaluated in each of them. Wine samples were presented in a balanced random order in coded glasses and were tasted in duplicate. Reference astringency solutions were provided in each session. The panelists tasted 30 mL of the wine in individual booths wearing a blindfold. They were advised to neutralize the oral cavity with water and bread and to wait 3 minutes before tasting the following sample.

### *Statistical analysis*

Statistical analysis of the results was performed using XLSTAT (Version 2014.4.06, AddinSoft Technologies, Paris, France). For pairwise comparisons, an ANOVA with a selected significance level of  $p < 0.05$  was used.

## **Results**

### *Wine samples and storage*

The two wines chosen for this study presented a similar initial composition and were stored at elevated temperature to accelerate reactions normally occurring during red wine aging. Two bottles of each wine were subjected to forced aging for three or six weeks. The results of the FT-IR analysis revealed only negligible changes in the wines' general composition after storage. The

color assessed by the CIELab parameters hue and chroma (Table 1), showed that the 2018 wines exhibited greater color intensities than the 2016 samples. In contrast to the rather high  $\Delta E$  values between fresh and stored samples of 4.66 and 8.93 for the 2016 and 2018 wines, respectively, the color differences were hardly perceptible. The higher  $\Delta E$  value of the 2018 wines may be explained by the faster loss of anthocyanins in younger wines due to the exponential decline of anthocyanins during aging (McRae et al. 2012).

Since color intensity is correlated with anthocyanin concentration and red wine maturity, the loss of color is consistent with the fast decline of anthocyanin concentrations during storage (Figure 1A). This development can be explained by the degradation, conversion, and incorporation of anthocyanins into pyranoanthocyanins and polymeric pigments, respectively. Figures 1B and 1C indicate higher proportions of polymeric pigments in the 2016 wines compared to the 2018 samples, whereby both contain more non-precipitable polymeric pigments (PP) than precipitable PP. While the proportion of precipitable PP is increasing in both samples, the amount of non-precipitable PP is increasing only in the 2018 wine. In the 2016 wine, non-precipitable PP concentration leveled, whereas in the 2018 wine, the non-precipitable PP concentration increased. While concentrations of precipitable PP increased, tannin concentrations decreased in the wine samples (Figure 1).

Since the wines did not show considerable differences in terms of sourness and bitterness, which was also proven by the FT-IR data, only wine astringency was further assessed in the sensory analysis. The sensory evaluation of the perceived astringency revealed that the 2016 wine appears to induce higher but still moderate astringency (Table 2). A four-way ANOVA of the

242 astringency rating including vintage, storage, panelist, and replicate is presented in Supplemental  
243 Table 1. The astringency of the wines slightly declined which is in line with the findings for tannin  
244 concentrations (Figure 1D). Interestingly, the astringency of the 3 weeks stored 2018 sample  
245 dropped to 3.5 but increased during another 3 weeks of storage. This coincides only partially with  
246 the tannin concentrations as tannin concentration declined constantly over time in the 2018 wine.

#### 247 *Isolation of a polyphenol rich extract and fractionation using silica gel*

248 The yields of the polyphenol rich extracts obtained by solid phase extraction using  
249 Amberlite XAD7 as solid phase were  $3.6 \pm 0.1$  g/L for the 2018 wines and  $4.1 \pm 0.1$  g/L for the 2016  
250 wines. For every wine sample, the low-pressure fractionation on silica gel was repeated 6 to 8  
251 times to produce enough material for the following analyses. The separation with silica gel  
252 primarily works on size exclusion, but hydrogen bonding between the phenolics and the silanol  
253 groups also plays an important role. The ternary isocratic separation of the injected extracts  
254 generated three fractions and the corresponding yields, and the distribution are given in Table 3.  
255 The elution of the fractions was monitored at 280 and 520 nm.

#### 256 *Composition of the FLASH fractions*

257 Table 1 presents the color metrics recorded for the fractions of all wine samples. With  
258 chroma values of 13 to 16 and a color hue of around 70, fractions 1 had a light orange to yellow  
259 coloration indicating a limited amount of red pigments. Having color hues of 28 and 35 each  
260 fraction 2 and 3 of the 2018 wine were closer to a blueish red color than fraction 2 and 3 of the  
261 2016 wine with values of 37 and 41, respectively.

The results of the protein precipitation assay (Figure 2A) show that the highest number of anthocyanins was found in fraction 2 of the 2018 wine. In all fractions, the amount of non-precipitable PP (Figure 2B) is higher than that of precipitable PP (Figure 2C) and tannins were only found in fractions 2 and 3. Tannins, polymeric pigments, and monomeric anthocyanins are absent in fraction 1, suggesting that fraction 1 is mainly composed of non-polar and non-phenolic substances.

Figure 3 presents the octanol water partitioning coefficients ( $K_{ow}$ ) of the fractions. A  $K_{ow}$  higher than 1 implies that the fraction is lipophilic, while values below 1 express the hydrophilicity of the contained compounds. The  $K_{ow}$  of the fractions follows the elution gradient of the FLASH separation as expected, where fraction 1 showed hydrophobic properties, while fractions 2 and 3 are both hydrophilic. The highest hydrophilicity is found in fraction 3 of both vintages. Merrell et al. (2018) determined the octanol water partitioning coefficients of young and aged Cabernet Sauvignon wines and defined coefficients of around 0.19 for young wines. This is comparable to the values found in this study for the wine extracts (Figure 3A).

The results of the UHPLC-MS analyses show that fraction 1 mainly contains gallic acid, monomeric flavan-3-ols, hydroxycinnamic acids and oligomeric procyanidins, whereas malvidin-3-*O*-glucoside is the main compound in fractions 2 and 3 (Supplemental Table 2 and 3). In agreement with the color and the precipitation assay, fraction 1 is characterized by the absence of anthocyanins and their derivatives.

*Changes in the fractions during wine storage*

The storage of the wines did not change the quantitative proportions of the fractions. Anthocyanins in fractions 2 and 3 declined in both vintages. The decrease in anthocyanins does not lead to a loss in color intensity (chroma), but goes along with a change in hue which indicates structural changes of pigments rather than a mere loss. Non-precipitable PP (Figure 2B) of the 2018 wine increased in fraction 2 and decreased in fraction 3. Since a less polar solvent elutes fraction 2, these developments of non-precipitable PP also indicate structural transformations of molecules, which correspond with declining polarities. In the 2016 wine, non-precipitable PP concentrations remained constant in both fractions. In fractions 2 and 3, precipitable PP (Figure 2C) increased during storage. No changes in tannin concentrations were detected except in fraction 2 of the 2016 wine, which showed a slight decrease indicating that the amount of less polar tannins of the 2016 wine decreased over time.

As a result of lower concentrations in polymeric pigments, the color of fraction 3 of the 2018 wine changed the most while the color of the other fractions (Table 1) was rather constant. It is apparent that the hydrophilicity of the fractions changed significantly during storage, however alterations are rather small with only fraction 3 of the 2018 wine undergoing considerable changes (Figure 3). Fraction 1 of the 2016 wine becomes more hydrophilic while fraction 1 of the 2018 wine shows higher hydrophobicity after storage. In fraction 2 of the 2016 wine and fraction 3 of the 2018 wine the hydrophilicity is increasing, whereas in fraction 3 of the 2016 wine and fraction 2 of the 2018 wine at the end of the 6 weeks storage no change was detected. Nevertheless, a rise

and a decrease of water solubility in fraction 3 of the 2016 wine and fraction 2 of the 2018 wine, respectively, occurred after 3 weeks.

In contrast to the anthocyanin concentrations, the UHPLC-MS results show no changes in the concentration of anthocyanin-derived pigments like pyranoanthocyanins or anthocyanin-flavanol oligomers (Supplemental Table 2 and 3). Likewise, monomeric flavanols, benzoic acids, hydroxycinnamic acids, flavanol dimers and trimers did not decrease.

## Discussion

This study was conducted to gain a deeper understanding of structural transformations of polyphenols occurring during forced red wine aging and their effects on astringency perception. Earlier studies (Boselli et al. 2004, Landon et al. 2008, Chira et al. 2011) associated red wine astringency with tannin concentrations as well as the vintage of the wines. Accordingly, the astringency of the 2018 wine was expected to be higher than that of the 2016 wine, and the wines were expected to decrease in astringency during forced aging; neither of which was actually observed (Table 2). This indicates that astringency is not only influenced by tannin concentrations but also by structural and compositional differences (Gawel 1998) like the degree of polymerization (Chira et al. 2012) and the composition of tannin sub-units, in particular their degree of galloylation and trihydroxylation on the B-ring (Vidal et al. 2003). According to Vidal et al. (2003) roughness of astringency increases with proceeding galloylation and decreases with the number of epigallocatechin subunits. To compare tannin concentration in the wines and extracts, the values obtained for the extracts were referenced to the corresponding volume of the wine considering the respective yield (Table 3). In contrast to the results obtained for the wines,

significantly higher tannin concentrations and no significant changes of tannin concentrations were found in the XAD7 extracts of the corresponding wines. These differences may be explained by interactions of the tannins with wine polysaccharides that are eliminated by the extraction procedure. The polysaccharides can form complexes with the tannins leading to an impaired precipitability with the BSA (Mateus et al. 2004) used for tannin quantification which results in lower tannin readings. Since the differences in tannin concentrations between wines and extracts increased, these interactions appear to become more pronounced when the wine is subjected to forced aging probably due to structural changes of the tannins. Precipitable PPs can be regarded as pigmented tannins since they are part of the tannin fraction determined after precipitation with BSA. The results show increasing precipitable PP ratios combined with decreasing or constant tannin levels indicating a progressive incorporation of anthocyanins into tannin molecules. Sommer et al. (2016) investigated the haze formation in red wines when treated with carboxymethyl cellulose (CMC). They found that CMC forms haze with wine proteins rather than with tannins and proposed a protein-bridged reaction between anthocyanins and CMC that leads to their precipitation. Accordingly, the incorporation of anthocyanins into tannin molecules changes the interaction between tannin sub-units and polysaccharides as well as proteins camouflaging them from analysis. Polysaccharides may also interact directly with BSA (de Freitas et al. 2003), which is used for tannin precipitation and might be another reason for the underestimation of tannins in wine samples. Astringency perception is also affected by wine polysaccharides that interact with red wine tannins and salivary proteins (Vidal et al. 2004b , Watrelot et al. 2017). Panelists were only requested to rate the overall astringency intensity that was compared to the drying mouthfeel evoked by aluminum sulfate. Future research should look



at the perception of different astringency sub-qualities to investigate whether the decrease of astringency rather represents a change in sub-qualities towards a less harsh mouthfeel. These results show that the tannin concentration may not be the only factor that should be considered for an evaluation of astringency and the sensory quality of the wine in general. Weber et al. (2013) showed that gel permeation chromatography fractions containing the highest number of polymeric pigments and rather small tannin concentrations elicited the lowest astringency as well as green and dry tannins intensity. A continuously increasing precipitable PP/tannin ratio of the wines may have favored the perception of a softer astringency.

The mechanism of astringency perception is based on tannin-protein interactions leading to insoluble precipitates, increasing friction and a loss of lubrication in the oral cavity (Baxter et al. 1997). Charlton et al. (2002) proposed a model for protein precipitation that is initially driven by hydrophobic interactions between the proline residues of proline-rich proteins and the aromatic flavonoid rings. These soluble aggregates are further stabilized through hydrogen bonding leading to cross linked tannin-protein complexes and their precipitation, suggesting that hydrophilicity is an important factor determining the astringency of distinct compounds.

The ratio of the concentration of lipophilic to hydrophilic compounds in the fractions is reflected by the octanol water partitioning coefficient ( $K_{OW}$ ). The generally higher anthocyanin concentrations in fraction 2 of all samples raised the expectation to observe higher hydrophilicities of this fraction compared with fraction 3. Since this was not the case, other compounds, like polymeric pigments and tannins, apparently contribute more to the overall hydrophilicity of the fractions. Hagerman et al. (1998) investigated the effect of growing tannin polymer lengths on the precipitability and the  $K_{OW}$ . They stated that tannins with higher degrees of polymerization

exhibited lower octanol water partitioning coefficients compared to their corresponding flavan-3-ol subunits. Hence, a higher degree of polymerization results in higher hydrophilic properties and precipitability. The hydrophobic character of fractions 1 is the result of the presence of monomeric flavan-3-ols, oligomeric procyanidins as well as benzoic and hydroxycinnamic acids.

The leveling concentrations of non-precipitable PP in fractions 2 and 3 of the 2016 wine lead to the assumption that the wines reached a maximum of non-precipitable PP which was already reported by Merrell et al. (2018) and may have two explanations. First, the formation and degradation processes of non-precipitable PP reached an equilibrium or, second, the formation of polymeric pigments in the older red wine that was subjected to forced aging favors the development of high molecular pigments that are not included into the non-precipitable PP measurement. Harbertson et al. (2014) showed that precipitation with BSA increases with polymer size of the tannins indicating that polymeric pigments that are resistant against SO<sub>2</sub> bleaching and that are not precipitated with BSA include oligomeric anthocyanin adducts as well as pyranoanthocyanins. The UHPLC-MS results show no considerable changes in the concentration of pyranoanthocyanins and anthocyanin-flavanol dimers (Supplemental Table 2 and 3). Hence, the protein precipitation assay indicates that anthocyanins are incorporated into existing polymeric structures to form polymeric pigments rather than forming new oligomeric pigments that grow in size. This is supported by earlier studies (Haslam 1980, Salas et al. 2003, Salas et al. 2004) that demonstrated that direct adducts of tannins and anthocyanins are formed after the preceding acid-catalyzed cleavage of procyanidins. The products formed during this reaction may still be regarded as polymeric structures although they might be of lower molecular weight due to the breakdown process.

The decline of tannins in fraction 2 of the 2016 wine together with a rise of precipitable PP results in the increase of hydrophilicity. This indicates that tannins initially found in fraction 2 of the 2016 wine are rather small and, thus, non-polar and hydrophobic, whereas the proceeding incorporation of anthocyanins during forced aging leads to more water soluble polymeric pigments (Singleton and Trousdale 1992, Merrell et al. 2018). Since the tannin concentration of fraction 3 of the 2016 wine remains constant, the corresponding partitioning coefficients follow the developments of precipitable PP, showing that fraction 3 of the 2016 wine contains large and polar tannins that were progressively pigmented during storage. In the 2018 wines, tannin concentrations in fractions 2 and 3 show no changes over time and accordingly, hydrophilicity seems to be affected by the compositional changes of precipitable PP and non-precipitable PP. As the determination of polymeric pigments is based on their absorption at 520 nm, the protein-precipitation assay does not distinguish between polymers of different intramolecular compositions (Weber et al. 2013). Hence, no conclusion can be drawn about the exact size of the molecules and the proportion of anthocyanins incorporated. Weber et al. (2013) examined the chemical composition of red wine polymers obtained by gel permeation chromatography that is based on the separation of molecules due to their size and polarity. Combining several analytical techniques, they stated that early eluting fractions were composed of large and less pigmented polymers. Further retention on the column eluted polymers with decreasing molecular size and increasing anthocyanin incorporation followed by less pigmented proanthocyanidin-like oligomers. Together with the results of the present study, the changes in hydrophilicity as well as the distribution of polymeric pigments between the fractions visualize the compositional transformations of red wine polymers. The hydrophilicity of fraction 2 of the 2018 wine decreased

during the first 3 weeks while the amount of precipitable PP increased. Because fraction 2 contains less polar and smaller polymers compared to fraction 3, this suggests an increase in the amount of smaller precipitable PP rather than an increase in the proportion of incorporated anthocyanins, i.e. the degree of pigmentation.

In contrast, the increase in hydrophilicity after 6 weeks resulted from the increase in non-precipitable PP or rather the augmented pigmentation of non-precipitable PP. The progressive increase in hydrophilicity of fraction 3 of the 2018 wine is caused by the ongoing new formation of larger precipitable PP or the continuous pigmentation of already existing large precipitable PP, and the simultaneous decrease of smaller non-precipitable PP that are less pigmented.

The different sub-qualities of astringency perception are explained by the varying manifestation of the physico-chemical interactions between tannins and proteins, which are specific and dependent on the molecular weight, the 3D structure and the water-solubility of tannins, that is, according to Haslam (1996), one of the main factors for tannin complexation (Simon et al. 2003). Being of a certain size, polyphenols can act as multidentate ligands binding more than one site of the protein (de Freitas and Mateus 2001) leading to the formation of protein-tannin networks and eventually precipitation (Cala et al. 2010). The formation of such networks and resulting astringent sensations were shown to be influenced by stereochemistry and conformation of procyanidins, because intramolecular stacking hinders the development of protein-tannin aggregates (Cala et al. 2010, Quijada-Morín et al. 2012). An earlier study (McRae et al. 2010) showed that the interactions between red wine tannins and a prolin-rich peptide changed with wine age towards less pronounced hydrophobic interactions. The authors attribute this to the change of tannin structures, like the incorporation of anthocyanins.

In 2013, McRae et al. showed that tannins obtained by liquid liquid extraction with butanol were smaller in size, more hydrophobic and comprise more red pigments than the aqueous fractions, which was inversely correlated with the perceived astringency. The findings of McRae et al. (2013), the results published by Weber et al. (2013), and the results of the present study argue for the concept of pigmented tannins being less astringent than non-pigmented tannins. Accordingly, a higher degree of pigmentation is not necessarily resulting in lower hydrophobicity since other structural features also contribute to the overall hydrophobicity of the tannins. The higher hydrophobicity of the butanol tannins may be due to a greater oxidation and an increased amount of intramolecular bonds possibly leading to a reduced number of binding sites, hence, a reduced astringency (McRae et al. 2013). The interim decline of astringency of the 2018 wine stored for 3 weeks might be the consequence of the considerably higher non-precipitable PP in fraction 2 and the increase in hydrophobicity of this fraction at this point of forced aging, while the further alterations of the tannins lead to an increase in astringency after 6 weeks of storage.

Finding tannins, PP in both, fraction 2 and fraction 3, indicates that not only the size of these polymers is important for their protein precipitability. It is affected by the physicochemical properties, which in turn depend on the size of tannin molecules and the ratio of incorporated anthocyanins, among others. However, it has still to be investigated how the elongation of polymers by anthocyanins as well as flavanols influences the protein precipitability.

## Conclusion

The present results reveal that a wide structural variety of pigments can be found within the classification of polymeric pigments into two categories. This variety is based on the differences

of sub-units as well as chain length and ratio of incorporated anthocyanins and leads to polymers of different physicochemical properties that can be visualized by the octanol-water partitioning coefficient and the FLASH fractionation. The change of polarity of polymeric pigments in turn alters their ability to interact with wine polysaccharides and saliva proteins. Since the presumed proceeding incorporation of anthocyanins into tannin molecules, which can be assumed by the presented increase in precipitable PP, appears to reduce the measurability of precipitable tannins during forced aging, a special role may be assigned to the interactions of precipitable PP with polysaccharides and proteins. The formation of precipitable PPs during forced red wine aging and their putative enhanced interactions with wine polysaccharides obviously play a key role in the perception of red wine astringency. In particular, the perception of different sub-qualities of astringency seems to be related to the proportion of precipitable PP and polysaccharides, which needs to be addressed in the course of continuing research.

### Literature Cited

- Adams DO, Harbertson JF, Picciotto EA. 2004. Fractionation of red wine polymeric pigments by protein precipitation and bisulfite bleaching. *In* Red Wine Color. AL Waterhouse and JA Kennedy (eds.), pp. 275–288. Am. Chem. Soc., Washington, DC.
- Baxter NJ, Lilley TH, Haslam E, Williamson MP. 1997. Multiple interactions between polyphenols and a salivary proline-rich protein repeat result in complexation and precipitation. *Biochemistry* 36:5566–5577.
- Bindon KA, McCarthy MG, Smith PA. 2014. Development of wine colour and non-bleachable pigments during the fermentation and ageing of (*Vitis vinifera* L. cv.) Cabernet Sauvignon wines differing in anthocyanin and tannin concentration. *LWT* 59:923–932.
- Boselli E, Boulton RB, Thorngate JH, Frega NG. 2004. Chemical and sensory characterization of DOC red wines from Marche (Italy) related to vintage and grape cultivars. *J. Agric. Food Chem.* 52:3843–3854.

- 479 Cala O, Pinaud N, Simon C, Fouquet E, Laguerre M, Dufourc EJ, Pianet I. 2010. NMR and molecular  
480 modeling of wine tannins binding to saliva proteins: revisiting astringency from molecular and  
481 colloidal prospects. *FASEB J.* 24:4281–4290.
- 482 Charlton AJ, Baxter NJ, Khan ML, Moir AJG, Haslam E, Davies AP, Williamson MP. 2002.  
483 Polyphenol/peptide binding and precipitation. *J. Agric. Food Chem.* 50:1593–1601.
- 484 Cheynier V, Dueñas-Paton M, Salas E, Maury C, Souquet J-M, Sarni-Manchado P, Fulcrand H. 2006.  
485 Structure and properties of wine Pigments and tannins. *Am J Enol Vitic* 57:298–305.
- 486 Chira K, Pacella N, Jourdes M, Teissedre P-L. 2011. Chemical and sensory evaluation of Bordeaux wines  
487 (Cabernet-Sauvignon and Merlot) and correlation with wine age. *Food Chem.* 126:1971–1977.
- 488 Chira K, Jourdes M, Teissedre P-L. 2012. Cabernet sauvignon red wine astringency quality control by  
489 tannin characterization and polymerization during storage. *Eur. Food Res. and Technol.* 234:253–  
490 261.
- 491 de Freitas V, Mateus N. 2001. Structural features of procyanidin interactions with salivary proteins. *J.*  
492 *Agric. Food Chem.* 49:940–945.
- 493 de Freitas V, Carvalho E, Mateus N. 2003. Study of carbohydrate influence on protein–tannin aggregation  
494 by nephelometry. *Food Chem.* 81:503–509.
- 495 Fulcrand H, Dueñas M, Salas E, Cheynier V. 2006. Phenolic reactions during winemaking and aging. *Am*  
496 *J Enol Vitic* 57:289–297.
- 497 Gawel R. 1998. Red wine astringency: A review. *Aust. J. Grape Wine Res.* 4:74–95.
- 498 Hagerman AE, Rice ME, Ritchard NT. 1998. Mechanisms of protein precipitation for two tannins,  
499 pentagalloyl glucose and epicatechin 16 (4→8) catechin (procyanidin). *J. Agric. Food Chem.*  
500 46:2590–2595.
- 501 Harbertson JF, Kennedy JA, Adams DO. 2002. Tannin in skins and seeds of Cabernet Sauvignon, Syrah,  
502 and Pinot noir berries during ripening. *Am J Enol Vitic* 53:54–59.
- 503 Harbertson JF, Picciotto EA, Adams DO. 2003. Measurement of polymeric pigments in grape berry extracts  
504 and wines using a protein precipitation assay combined with bisulfite bleaching. *Am J Enol Vitic*  
505 54:301–306.
- 506 Harbertson JF, Mireles MS, Harwood ED, Weller KM, Ross CF. 2009. Chemical and sensory effects of  
507 saignée, water addition, and extended maceration on high Brix must. *Am J Enol Vitic* 60:450–460.
- 508 Harbertson JF, Kilmister RL, Kelm MA, Downey MO. 2014. Impact of condensed tannin size as individual  
509 and mixed polymers on bovine serum albumin precipitation. *Food Chem.* 160:16–21.
- 510 Harbertson JF, Mireles M, Yu Y. 2015. Improvement of BSA tannin precipitation assay by reformulation  
511 of resuspension buffer. *Am J Enol Vitic* 66:95–99.
- 512 Haslam E. 1980. In vino veritas: Oligomeric procyanidins and the ageing of red wines. *Phytochemistry*  
513 19:2577–2582.

- 514 Haslam E. 1996. Natural polyphenols (vegetable tannins) as drugs: Possible modes of action. *J. Nat. Prod.*  
515 59:205–215.
- 516 Kennedy JA, Jones GP. 2001. Analysis of proanthocyanidin cleavage products following acid-catalysis in  
517 the presence of excess phloroglucinol. *J. Agric. Food Chem.* 49:1740–1746.
- 518 Landon JL, Weller K, Harbertson JF, Ross CF. 2008. Chemical and sensory evaluation of astringency in  
519 Washington State red wines. *Am J Enol Vitic* 59:153–158.
- 520 Ma W, Waffo-Tégou P, Alessandra Pissoni M, Jourdes M, Teissedre P-L. 2018. New insight into the  
521 unresolved HPLC broad peak of Cabernet Sauvignon grape seed polymeric tannins by combining  
522 CPC and Q-ToF approaches. *Food Chem.* 249:168–175.
- 523 Mateus N, Carvalho E, Luís C, de Freitas V. 2004. Influence of the tannin structure on the disruption effect  
524 of carbohydrates on protein–tannin aggregates. *Anal. Chim. Acta* 513:135–140.
- 525 McRae JM, Falconer RJ, Kennedy JA. 2010. Thermodynamics of grape and wine tannin interaction with  
526 polyproline: Implications for red wine astringency. *J. Agric. Food Chem.* 58:12510–12518.
- 527 McRae JM, Dambergs RG, Kassara S, Parker M, Jeffery DW, Herderich MJ, Smith PA. 2012. Phenolic  
528 compositions of 50 and 30 year sequences of Australian red wines: The impact of wine age. *J.*  
529 *Agric. Food Chem.* 60:10093–10102.
- 530 McRae JM, Schulkin A, Kassara S, Holt HE, Smith PA. 2013. Sensory properties of wine tannin fractions:  
531 implications for in-mouth sensory properties. *J. Agric. Food Chem.* 61:719–727.
- 532 Merrell CP, Larsen RC, Harbertson JF. 2018. Effects of berry maturity and wine alcohol on phenolic content  
533 during winemaking and aging. *Am J Enol Vitic* 69:1–11.
- 534 Noble AC. 1998. Why do wines taste bitter and feel astringent? *In* *Chemistry of Wine Flavor*. AL  
535 Waterhouse and SE Ebeler (eds.), pp. 156–165. Am. Chem. Soc., Washington, DC.
- 536 OIV. 2006. Determination of chromatic characteristics according to CIELab. Resolution Oeno 1/2006 OIV,  
537 Paris, France.
- 538 Quijada-Morín N, Regueiro J, Simal-Gándara J, Tomás E, Rivas-Gonzalo JC, Escribano-Bailón MT. 2012.  
539 Relationship between the sensory-determined astringency and the flavanolic composition of red  
540 wines. *J. Agric. Food Chem.* 60:12355–12361.
- 541 Remy S, Fulcrand H, Labarbe B, Cheynier V, Moutounet M. 2000. First confirmation in red wine of  
542 products resulting from direct anthocyanin–tannin reactions. *J. Sci. Food Agric.* 80:745–751.
- 543 Salas E, Fulcrand H, Meudec E, Cheynier V. 2003. Reactions of anthocyanins and tannins in model  
544 solutions. *J. Agric. Food Chem.* 51:7951–7961.
- 545 Salas E, Atanasova V, Poncet-Legrand C, Meudec E, Mazauric JP, Cheynier V. 2004. Demonstration of  
546 the occurrence of flavanol–anthocyanin adducts in wine and in model solutions. *Anal. Chim. Acta*  
547 513:325–332.



- 548 Sarneckis CJ, Dambergs RG, Jones P, Mercurio M, Herderich MJ, Smith PA. 2006. Quantification of  
549 condensed tannins by precipitation with methyl cellulose: development and validation of an  
550 optimised tool for grape and wine analysis. *Aust. J. Grape Wine Res.* 12:39–49.
- 551 Simon C, Barathieu K, Laguerre M, Schmitter J-M, Fouquet E, Pianet I, Dufourc EJ. 2003. Three-  
552 Dimensional structure and dynamics of wine tannin–saliva protein complexes. A multitechnique  
553 approach. *Biochemistry* 42:10385–10395.
- 554 Singleton VL, Trousdale EK. 1992. Anthocyanin-tannin interactions explaining differences in polymeric  
555 phenols between white and red wines. *Am J Enol Vitic* 43:63–70.
- 556 Sommer S, Dickescheid C, Harbertson JF, Fischer U, Cohen SD. 2016. Rationale for haze formation after  
557 carboxymethyl cellulose (CMC) addition to red wine. *J. Agric. Food Chem.* 64:6879–6887.
- 558 Vidal S, Francis L, Guyot S, Marnet N, Kwiatkowski M, Gawel R, Cheynier V, Waters EJ. 2003. The  
559 mouth-feel properties of grape and apple proanthocyanidins in a wine-like medium. *J. Sci. Food*  
560 *Agric.* 83:564–573.
- 561 Vidal S, Francis L, Noble A, Kwiatkowski M, Cheynier V, Waters E. 2004a. Taste and mouth-feel  
562 properties of different types of tannin-like polyphenolic compounds and anthocyanins in wine.  
563 *Anal. Chim. Acta* 513:57–65.
- 564 Vidal S, Francis L, Williams P, Kwiatkowski M, Gawel R, Cheynier V, Waters E. 2004b. The mouth-feel  
565 properties of polysaccharides and anthocyanins in a wine like medium. *Food Chem.* 85:519–525.
- 566 Watrelot AA, Schulz DL, Kennedy JA. 2017. Wine polysaccharides influence tannin-protein interactions.  
567 *Food Hydrocoll.* 63:571–579.
- 568 Weber F, Greve K, Durner D, Fischer U, Winterhalter P. 2013. Sensory and chemical characterization of  
569 phenolic polymers from red wine obtained by gel permeation chromatography. *Am J Enol Vitic*  
570 64:15–25.
- 571

**Table 1** CIELab parameters of Cabernet Sauvignon wines and silica gel fractions at the various stages of storage at 35°C.

Sample	Wine			Fraction 1		Fraction 2		Fraction 3	
	weeks	h°	C*	h°	C*	h°	C*	h°	C*
2016	0	14.97	29.12	69.82	15.21	36.23	53.21	40.39	45.44
	3	15.88	23.94	72.84	15.96	37.36	53.08	40.67	47.99
	6	16.13	24.62	72.84	13.80	37.81	52.22	42.75	46.86
2018	0	20.17	38.88	70.18	14.52	27.36	50.47	32.56	47.08
	3	17.6	30.1	71.16	13.09	28.44	51.15	35.19	41.75
	6	18.07	30.54	71.49	13.60	29.54	51.33	37.25	42.29

**Table 2** Astringency ratings (left) of Cabernet Sauvignon wines at the various stages of storage at 35°C (means presented with standard deviation; n = 14;). Means within columns and between tannin concentrations having the same letters are not significantly different at  $p \leq 0.05$ . Tannin concentrations of the wines and the corresponding extracts (right); means presented with standard deviation; n = 3; Concentrations with different capital letters are significantly different between the wines and the extracts ( $p \leq 0.05$ ).

Sample	Weeks	Wine	Extract
		Astringency	Tannins (mg/L CE)
2016	0	6.52 ± 1.50 a	692.05 ± 3.24 B
	3	6.27 ± 1.86 ab	669.48 ± 20.68 BC
	6	5.46 ± 2.48 ab	654.98 ± 12.39 C
2018	0	5.50 ± 2.13 ab	607.66 ± 4.15 D
	3	3.56 ± 1.09 c	535.39 ± 18.45 E
	6	4.53 ± 1.47 bc	508.49 ± 8.64 E

**Table 3** Yields and proportions (in parentheses) of silica gel chromatography fractions of Cabernet Sauvignon XAD7 extracts after storage at 35°C (means presented with standard deviation; n = 6-8).

Sample	2016			2018		
	Yield (mg/g) (Proportion (%))					
Weeks	0	3	6	0	3	6
F1	130.2 ± 29.4	162.2 ± 0.8	162.1 ± 3.7	154.0 ± 45.1	158.7 ± 39.7	145.9 ± 44.5
	(21.0 ± 4.7)	(25.1 ± 0.2)	(24.9 ± 0.6)	(24.8 ± 7.2)	(23.4 ± 5.9)	(21.7 ± 6.6)
F2	396.8 ± 6.8	368.4 ± 31.6	378.7 ± 12.4	421.2 ± 29.1	450.4 ± 2.3	451.1 ± 71.2
	(64.0 ± 1.2)	(57.0 ± 4.5)	(58.1 ± 1.9)	(67.7 ± 4.7)	(66.4 ± 0.3)	(67.1 ± 10.6)
F3	93.4 ± 10.8	114.6 ± 39.9	112.6 ± 8.4	48.3 ± 17.8	70.1 ± 19.4	75.7 ± 20.7
	(15.1 ± 3.8)	(17.7 ± 5.8)	(17.3 ± 1.3)	(7.8 ± 2.9)	(10.3 ± 2.9)	(11.3 ± 3.1)

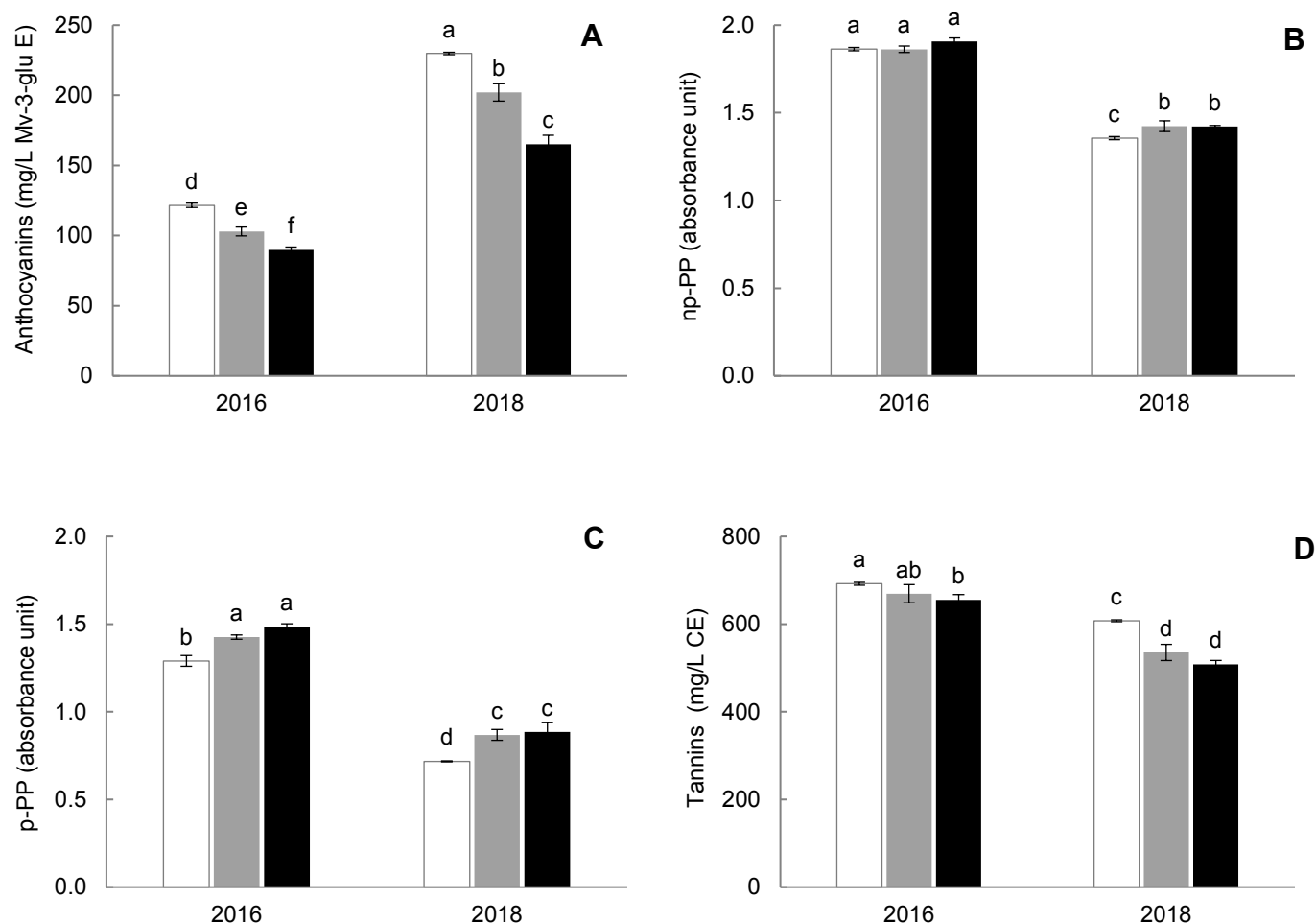


**Figure 1** Phenolic composition including total anthocyanins (**A**), non-precipitable polymeric pigments (np-PP; **B**), precipitable polymeric pigments (p-PP; **C**), and total tannins (**D**) of Cabernet Sauvignon wines at the various stages of storage at 35°C: no storage (□), 3 weeks (▒), and 6 weeks (■). Results obtained by photometric assays (Harbertson et al. 2002, 2003, 2009, 2015). Means presented with standard deviation; n = 3. Means having the same letters are not significantly different at  $p \leq 0.05$ .

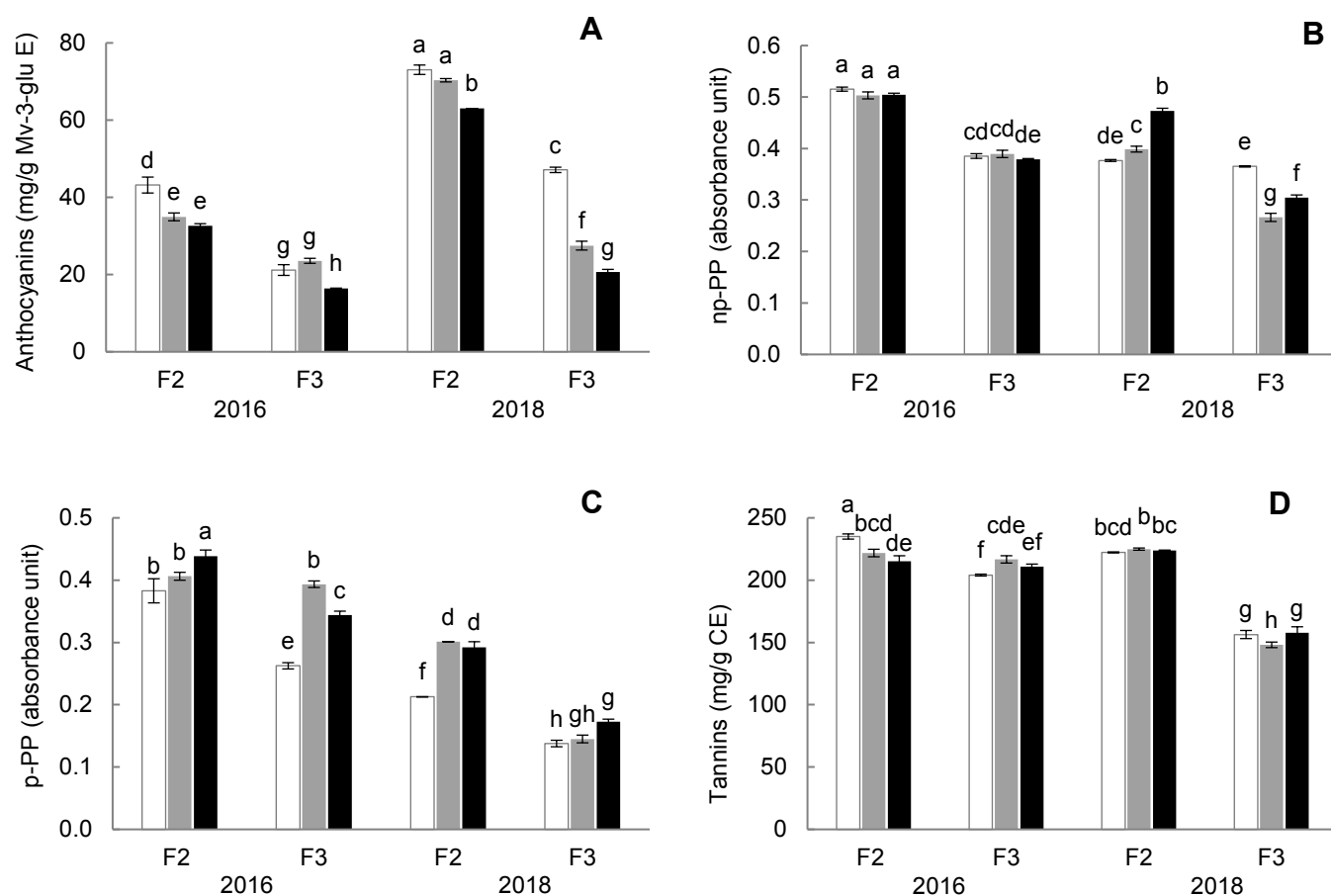


**Figure 2** Phenolic composition including total anthocyanins (**A**), non-precipitable polymeric pigments (np-PP; **B**), precipitable polymeric pigments (p-PP; **C**), and total tannins (**D**) of silica gel chromatography fraction 2 (F2) and fraction 3 (F3) of Cabernet Sauvignon XAD7 extracts at the various stages of storage at 35°C: no storage (□), 3 weeks (■), and 6 weeks (■). Results obtained by photometric assays (Harbertson et al. 2002, 2003, 2009, 2015). Means presented with standard deviation; n = 3. Means having the same letters are not significantly different at  $p \leq 0.05$ .

**Figure 3**

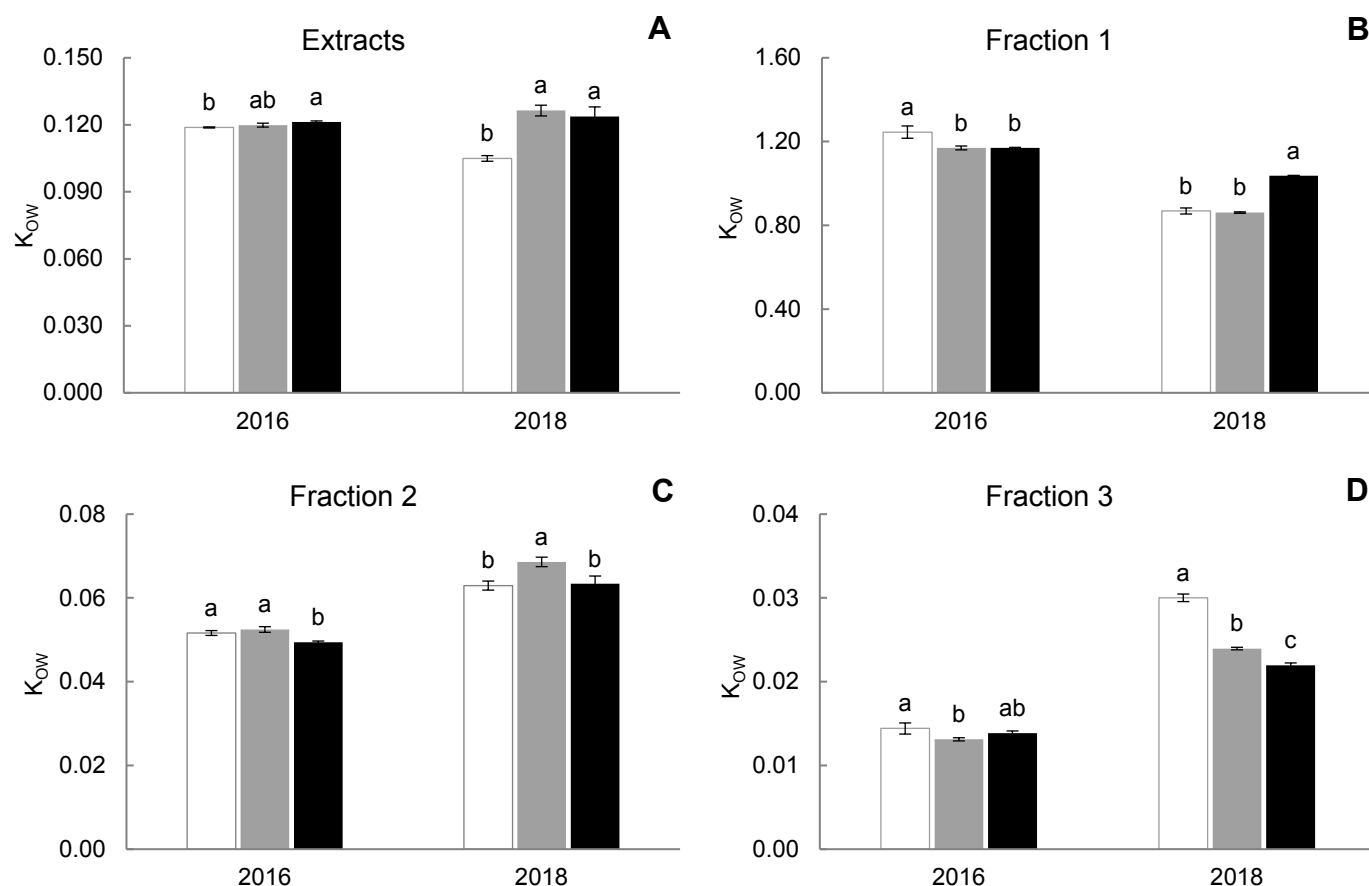


**Figure 3** Octanol water partitioning coefficients ( $K_{ow}$ ) of XAD7 extracts (A), and silica gel chromatography fraction 1 (B), fraction 2 (C), and fraction 3 (D) of Cabernet Sauvignon wines at the various stages of storage at 35°C: no storage (□), 3 weeks (■), and 6 weeks (■). Means presented with standard deviation;  $n = 3$ . Means within columns having the same letters are not significantly different at  $p \leq 0.05$ .

**Supplemental Table 1** Fourway-ANOVA of the astringency rating including vintage, storage, panelist, and replicate of the tasting showing that the vintage of the wines and the panelist have a significant impact on the astringency rating at  $p \leq 0.05$ .

Source	Degrees of freedom	Sum of squares	Mean of squares	F-value	p-value
Vintage	1	48.747	48.747	12.861	0.000
Storage	2	20.859	10.430	2.752	0.068
Panelist	13	100.143	7.703	2.032	0.023
Replicate	1	0.547	0.547	0.144	0.705

**Supplemental Table 2** Heat map of the low molecular phenolic composition of 2016 Cabernet Sauvignon wine fractions at the various stages of storage at 35°C determined with UHPLC-MS/MS. Means presented with mean standard deviation (mSD) for substance classes, n = 3.

Substance (mg/g)	Fraction 1			Fraction 2			Fraction 3		
weeks	0	3	6	0	3	6	0	3	6
<i>Anthocyanins</i> ( $\pm 0.06$ mSD)									
Delphinidin-3-glucoside	n.d.	n.d.	n.d.	0.39	0.36	0.27	0.62	0.44	0.41
Cyanidin-3-glucoside	n.d.	n.d.	n.d.	0.07	0.06	0.05	0.06	0.03	0.03
Petunidin-3-glucoside	n.d.	n.d.	n.d.	0.92	0.78	0.62	0.73	0.56	0.50
peonidin-3-glucoside	n.d.	n.d.	n.d.	0.89	0.68	0.61	0.22	0.22	0.15
Malvidin-3-glucoside	n.d.	n.d.	n.d.	13.06	9.46	9.00	4.16	4.05	2.79
Delphinidin-3-(6-acetyl)glucoside	n.d.	n.d.	n.d.	0.09	0.09	0.06	0.18	0.12	0.11
Petunidin-3-O-(6-O-acetyl)glucoside	n.d.	n.d.	n.d.	0.28	0.23	0.18	0.23	0.16	0.14
Malvidin Formiat	n.d.	n.d.	n.d.	0.28	0.26	0.26	0.12	0.08	0.06
Peonidin 3-O-acetylglucoside	n.d.	n.d.	n.d.	0.40	0.28	0.24	0.07	0.07	0.04
Delphinidin-3-(p-coumaroyl)glucoside	n.d.	n.d.	n.d.	n.d.	n.d.	n.d.	n.d.	n.d.	n.d.
Malvidin-3-O-(6-O-acetyl)glucoside	n.d.	n.d.	n.d.	5.43	3.95	3.36	1.23	1.15	0.80
Petunidin-3-(p-coumaroyl)glucoside cis	n.d.	n.d.	n.d.	n.d.	n.d.	n.d.	0.04	n.d.	n.d.
Petunidin-3-(p-coumaroyl)glucoside trans	n.d.	n.d.	n.d.	0.06	0.05	0.04	n.d.	n.d.	n.d.
Malvidin-3-O-(6-O-p-coumaroyl)glucoside cis	n.d.	n.d.	n.d.	0.08	0.05	0.05	n.d.	n.d.	n.d.
Peonidin-3-(6"-p-coumaroyl)glucoside)	n.d.	n.d.	n.d.	0.14	0.10	0.09	n.d.	n.d.	n.d.
Malvidin-3-O-(6-O-p-coumaroyl)glucoside trans	n.d.	n.d.	n.d.	1.16	0.83	0.76	0.22	0.22	0.17
<i>Pyrananthocyanins</i> ( $\pm 0.01$ mSD)									
Petunidin-3-glucoside pyruvate (Vitisin A)	n.d.	n.d.	n.d.	0.05	0.05	0.05	0.04	0.04	0.04
Peonidin-3-glucoside pyruvate (Vitisin A)	n.d.	n.d.	n.d.	0.05	0.05	0.05	n.d.	n.d.	n.d.
Malvidin-3-O-glucosid pyruvate (Vitisin A)	n.d.	n.d.	n.d.	0.23	0.20	0.20	0.10	0.11	0.11



Malvidin-3-O-acetylglucoside pyruvate (Vitisin A)	n.d.	n.d.	n.d.	0.16	0.15	0.16	n.d.	n.d.	n.d.
Malvidin-3-glucoside-vinyl-catechin	n.d.	n.d.	n.d.	0.06	0.05	0.06	n.d.	n.d.	n.d.
Mv-3-glc-4-vinylcatechol (Pinotin)	n.d.	n.d.	n.d.	0.50	0.49	0.59	0.23	0.28	0.29
Malvidin-3-glucoside-vinyl-epicatechin	n.d.	n.d.	n.d.	0.09	0.08	0.09	n.d.	n.d.	n.d.
Malvidin-3-glucoside-4-vinylphenol (Pinotin)	n.d.	n.d.	n.d.	0.53	0.84	0.55	0.13	0.32	0.23
<i>Anthocyanin flavanol adducts (<math>\pm 0.01</math> mSD)</i>									
Malvidin-3-glucoside-gallocatechin	n.d.	n.d.	n.d.	0.23	0.21	0.20	0.06	0.05	0.04
Peonidin-3-glucoside-(epi)catechin	n.d.	n.d.	n.d.	0.08	0.08	0.07	n.d.	n.d.	n.d.
Malvidin-glucoside-(epi)catechin	n.d.	n.d.	n.d.	0.75	0.73	0.68	0.17	0.19	0.15
Malvedin-acetylglucoside-(epi)catechin	n.d.	n.d.	n.d.	0.13	0.12	0.11	n.d.	n.d.	n.d.
Malvidin-coumaroylglucoside-(epi)catechin	n.d.	n.d.	n.d.	0.06	0.06	0.05	n.d.	n.d.	n.d.
<i>Flavanols (<math>\pm 0.87</math> mSD)</i>									
Catechingallat	1.89	2.02	2.61	0.98	0.70	0.48	0.52	0.45	0.30
(-)-Gallocatechin	7.57	6.08	9.67	0.71	0.92	0.64	0.18	0.15	0.15
Epicatechingallat	1.29	1.13	1.63	0.70	0.43	0.34	n.d.	n.d.	n.d.
(-)-Epigallocatechin	2.57	1.89	2.75	0.16	0.18	0.12	0.05	0.04	0.04
Catechin	48.55	38.99	48.28	3.31	4.11	2.47	1.02	0.96	0.85
Epicatechin	33.78	23.75	28.66	1.80	2.28	1.54	0.72	0.65	0.62
<i>Proanthocyanidins (<math>\pm 0.30</math> mSD)</i>									
Flavanol trimer	0.60	0.50	0.58	0.42	0.18	0.15	0.37	0.32	0.29
Flavanol dimer	12.59	11.04	14.65	3.60	2.59	1.94	0.99	0.96	0.78
Flavanol dimer	4.04	3.19	4.47	0.54	0.38	0.23	0.05	0.07	0.06
Flavanol trimer	1.31	1.31	1.86	0.71	0.44	0.35	0.09	0.08	0.07
Flavanol trimer	0.99	1.10	1.61	0.43	0.30	0.22	0.03	0.03	0.03
Flavanol dimer	2.74	1.93	2.33	0.23	0.17	0.11	n.d.	n.d.	n.d.
Flavanol trimer	0.85	0.90	1.25	0.42	0.25	0.20	n.d.	n.d.	n.d.

Flavanol dimer	13.85	10.12	13.80	2.23	1.59	1.17	0.58	0.56	0.46
Flavanol dimer gallat	0.07	0.18	0.23	0.16	0.15	0.13	n.d.	n.d.	n.d.
Flavanol dimer gallat	0.02	0.06	0.09	0.09	0.09	0.07	n.d.	n.d.	n.d.
Flavanol trimer	1.69	1.54	2.08	0.52	0.32	0.22	0.07	0.06	0.05
<i>Flavonols (<math>\pm 0.23</math> mSD)</i>									
Dihydromyricetin-3-rhamnoside	0.10	0.14	0.19	0.17	0.15	0.12	n.d.	n.d.	n.d.
Myricetin-3-glucuronide	0.13	0.18	0.18	2.00	1.98	2.00	n.d.	n.d.	n.d.
Quercetin-3-O-glucuronide	0.91	1.23	1.19	4.99	3.95	4.31	0.60	0.50	0.57
Laricitrin-3-galactoside	n.d.	n.d.	n.d.	0.22	0.14	0.13	n.d.	n.d.	n.d.
Syringetin-3-glucoside	0.03	0.05	0.05	3.01	2.16	2.04	0.46	0.41	0.44
<i>Benzoic acids (<math>\pm 1.49</math> mSD)</i>									
Gallic acid	62.69	53.79	70.25	4.05	4.13	3.77	0.55	0.61	0.85
Vanillic acid	1.81	1.31	1.62	n.d.	n.d.	n.d.	n.d.	n.d.	n.d.
<i>Hydroxycinnamic acids (<math>\pm 0.35</math> mSD)</i>									
Cis-Caftaric acid	0.97	1.38	1.16	0.29	0.20	0.15	n.d.	n.d.	n.d.
Cis-Caffeic acid	6.16	5.17	5.77	2.42	2.03	1.89	n.d.	n.d.	n.d.
Trans-Caftaric acid	6.92	5.73	6.74	2.34	1.85	1.81	0.12	0.12	0.14
Hydroxy-caffeic acid dimer isomer	1.73	1.56	1.39	0.68	0.59	0.61	n.d.	n.d.	n.d.
Ferulic acid	0.85	0.55	0.83	n.d.	n.d.	n.d.	n.d.	n.d.	n.d.
cis-Coutaric acid	1.94	1.52	1.74	0.43	0.33	0.30	n.d.	n.d.	n.d.
p-Coumaric acid	13.64	11.81	13.69	n.d.	n.d.	n.d.	n.d.	n.d.	n.d.
trans-Coutaric acid	7.00	5.41	8.06	1.09	0.88	0.80	0.06	0.06	0.06
Trans-Caffeic acid	18.10	13.51	17.13	0.26	0.26	0.20	n.d.	n.d.	n.d.
cis-Ethylcaffeic acid	2.72	2.25	2.28	n.d.	n.d.	n.d.	n.d.	n.d.	n.d.

**Supplemental Table 3** Heat map of the low molecular phenolic composition of 2018 Cabernet Sauvignon wine fractions at the various stages of storage at 35°C determined with UHPLC-MS/MS. Means presented with mean standard deviation (mSD) for substance classes, n = 3.

Substance (mg/g)	Fraction 1			Fraction 2			Fraction 3		
weeks	0	3	6	0	3	6	0	3	6
<i>Anthocyanins</i> ( $\pm 0.06$ mSD)									
Delphinidin-3-glucoside	n.d.	n.d.	n.d.	0.62	0.54	0.44	2.73	1.09	0.94
Cyanidin-3-glucoside	n.d.	n.d.	n.d.	0.13	0.11	0.09	0.32	0.12	0.08
Petunidin-3-glucoside	n.d.	n.d.	n.d.	2.20	1.81	1.49	5.12	1.92	1.41
peonidin-3-glucoside	n.d.	0.05	n.d.	3.66	2.82	2.29	1.14	0.66	0.57
Malvidin-3-glucoside	0.06	0.37	0.03	30.00	26.71	22.49	12.78	8.34	7.99
Delphinidin-3-(6-acetyl)glucoside	n.d.	n.d.	n.d.	0.10	0.08	0.07	0.55	0.21	0.19
Petunidin-3-O-(6-O-acetyl)glucoside	n.d.	n.d.	n.d.	0.45	0.36	0.30	1.06	0.42	0.30
Malvidin Formiat	n.d.	n.d.	n.d.	0.82	1.00	0.65	0.23	0.15	0.13
Peonidin 3-O-acetylglucoside	0.03	0.04	n.d.	1.23	0.95	0.75	0.32	0.20	0.15
Delphinidin-3-(p-coumaroyl)glucoside	n.d.	n.d.	n.d.	0.13	0.11	0.09	0.42	0.19	0.12
Malvidin-3-O-(6-O-acetyl)glucoside	0.20	0.31	0.17	13.69	11.25	9.36	3.73	2.83	2.18
Petunidin-3-(p-coumaroyl)glucoside cis	n.d.	n.d.	n.d.	n.d.	n.d.	n.d.	0.67	0.29	0.17
Petunidin-3-(p-coumaroyl)glucoside trans	n.d.	n.d.	n.d.	0.44	0.33	0.27	n.d.	n.d.	n.d.
Malvidin-3-O-(6-O-p-coumaroyl)glucoside cis	n.d.	n.d.	n.d.	0.59	0.39	0.29	0.13	0.10	0.06
Peonidin-3-(6"-p-coumaroyl)glucoside)	n.d.	n.d.	n.d.	0.89	0.77	0.58	0.20	0.15	0.10
Malvidin-3-O-(6-O-p-coumaroyl)glucoside trans	n.d.	n.d.	n.d.	6.99	5.74	4.56	1.50	1.21	0.88
<i>Pyrananthocyanins</i> ( $\pm 0.01$ mSD)									
Petunidin-3-glucoside pyruvate (Vitisin A)	n.d.	n.d.	n.d.	0.04	0.04	0.03	0.13	0.04	0.03
Peonidin-3-glucoside pyruvate (Vitisin A)	n.d.	n.d.	n.d.	0.04	0.05	0.04	n.d.	n.d.	n.d.
Malvidin-3-O-glucosid pyruvate (Vitisin A)	n.d.	n.d.	n.d.	0.22	0.19	0.19	0.09	0.09	0.08

Malvidin-3-O-acetylglucoside pyruvate (Vitisin A)	n.d.	n.d.	n.d.	0.15	0.15	0.14	n.d.	n.d.	n.d.
Malvidin-3-glucoside-vinyl-catechin	n.d.	n.d.	n.d.	0.05	0.05	0.05	n.d.	n.d.	n.d.
Mv-3-glc-4-vinylcatechol (Pinotin)	n.d.	n.d.	n.d.	0.09	0.15	0.18	0.19	0.11	0.09
Malvidin-3-glucoside-vinyl-epicatechin	n.d.	n.d.	n.d.	0.08	0.08	0.07	n.d.	n.d.	n.d.
Malvidin-3-glucoside-4-vinylphenol (Pinotin)	n.d.	n.d.	n.d.	0.69	1.15	0.75	0.47	0.15	0.20
<i>Anthocyanin flavanol adducts (<math>\pm 0.01</math> mSD)</i>									
Malvidin-3-glucoside-gallocatechin	n.d.	n.d.	n.d.	0.28	0.32	0.29	0.11	0.07	0.06
Peonidin-3-glucoside-(epi)catechin	n.d.	n.d.	n.d.	0.14	0.16	0.14	0.07	0.04	0.04
Malvidin-glucoside-(epi)catechin	n.d.	n.d.	n.d.	0.86	1.07	0.91	0.36	0.24	0.25
Malvedin-acetylglucoside-(epi)catechin	n.d.	n.d.	n.d.	0.19	0.21	0.18	0.05	0.04	0.04
Malvidin-coumaroylglucoside-(epi)catechin	n.d.	n.d.	n.d.	0.16	0.20	0.17	0.05	0.04	0.04
<i>Flavanols (<math>\pm 0.87</math> mSD)</i>									
Catechingallat	3.26	3.27	3.26	1.55	1.44	1.05	0.47	0.97	0.71
(-)-Gallocatechin	9.01	6.67	8.16	0.94	1.01	0.70	0.23	0.14	0.13
Epicatechingallat	2.38	2.03	1.87	1.07	0.99	0.67	n.d.	n.d.	n.d.
(-)-Epigallocatechin	2.79	2.55	2.69	0.18	0.21	0.15	0.06	0.04	0.04
Catechin	56.66	51.39	55.98	3.87	4.33	3.59	1.32	0.90	0.86
Epicatechin	47.43	36.74	39.62	2.62	2.45	1.90	1.12	0.67	0.64
<i>Proanthocyanidins (<math>\pm 0.30</math> mSD)</i>									
Flavanol trimer	1.32	1.41	1.04	0.87	0.83	0.44	0.35	0.37	0.38
Flavanol dimer	20.22	18.91	18.54	6.49	6.96	4.43	1.98	1.01	1.04
Flavanol dimer	6.97	5.98	5.32	1.18	1.13	0.67	0.13	0.06	0.06
Flavanol trimer	3.36	2.87	2.81	1.50	1.31	0.87	0.22	0.09	0.09
Flavanol trimer	2.47	2.27	2.06	0.87	0.81	0.65	0.08	0.05	0.04
Flavanol dimer	5.45	3.90	3.98	0.62	0.54	0.29	0.08	0.06	0.07
Flavanol trimer	1.74	1.56	1.51	0.67	0.64	0.52	n.d.	n.d.	n.d.

Flavanol dimer	19.64	17.54	17.33	4.44	3.86	2.65	1.18	0.64	0.60
Flavanol dimer gallat	0.25	0.44	0.39	0.34	0.37	0.30	0.06	0.03	0.03
Flavanol dimer gallat	0.10	0.19	0.16	0.18	0.20	0.18	n.d.	n.d.	n.d.
Flavanol trimer	3.91	3.35	3.22	1.28	1.04	0.69	0.20	0.08	0.08
<i>Flavonols (<math>\pm 0.23</math> mSD)</i>									
Dihydromyricetin-3-rhamnoside	0.05	0.07	0.07	0.09	0.08	0.06	n.d.	n.d.	n.d.
Myricetin-3-glucuronide	0.30	0.43	0.26	2.70	2.18	2.03	n.d.	n.d.	n.d.
Quercetin-3-O-glucuronide	11.28	11.22	8.32	25.36	22.56	19.87	6.31	4.86	3.98
Laricitrin-3-galactoside	0.03	0.14	0.03	0.90	0.79	0.62	0.20	0.12	0.10
Syringetin-3-glucoside	0.08	0.57	0.10	3.64	3.49	2.80	0.85	0.68	0.55
<i>Benzoic acids (<math>\pm 1.49</math> mSD)</i>									
Gallic acid	67.91	65.59	66.14	4.68	3.96	3.12	1.85	0.63	0.74
Vanillic acid	3.05	3.19	3.10	n.d.	n.d.	n.d.	n.d.	n.d.	n.d.
<i>Hydroxycinnamic acids (<math>\pm 0.35</math> mSD)</i>									
Cis-Caftaric acid	2.70	1.16	0.62	0.54	0.41	0.18	0.04	0.08	0.04
Cis-Caffeic acid	8.85	9.32	10.49	2.55	2.73	2.15	n.d.	n.d.	n.d.
Trans-Caftaric acid	10.72	10.68	11.94	2.90	2.90	2.34	0.47	0.22	0.22
Hydroxy-caffeic acid dimer isomer	1.55	1.90	1.65	0.46	0.59	0.43	n.d.	n.d.	n.d.
Ferulic acid	0.95	0.95	0.99	n.d.	n.d.	n.d.	n.d.	n.d.	n.d.
cis-Coutaric acid	3.33	2.72	2.68	0.65	0.64	0.38	0.08	0.04	0.04
p-Coumaric acid	14.11	14.46	14.75	n.d.	n.d.	n.d.	n.d.	n.d.	n.d.
trans-Coutaric acid	9.27	7.73	8.93	1.10	1.05	0.75	0.15	0.07	0.07
Trans-Caffeic acid	15.89	15.10	15.00	0.16	0.09	0.08	n.d.	n.d.	n.d.
cis-Ethylcaffeic acid	2.33	2.44	2.40	n.d.	n.d.	n.d.	n.d.	n.d.	n.d.